Available online at www.sciencedirect.com
ScienceDirect
Tetrahedron Letters
Tetrahedron Letters 48 (2007) 3563–3567

Synthesis, electronic, and photophysical properties of cruciform OPE/OPV hybrid oligomer bridged bisfullerene triads

Ningzhang Zhou, Li Wang, David W. Thompson* and Yuming Zhao*

Department of Chemistry, Memorial University of Newfoundland, St. John's, NL, Canada A1B 3X7

Received 11 January 2007; revised 9 March 2007; accepted 17 March 2007
Available online 21 March 2007

Abstract—A series of cruciform-shaped phenyleneethynylene and phenylenevinylene hybrid oligomers was prepared via a sequence of Sonogashira reactions. Using an in situ ethynylation protocol, these oligomers were end-functionalized with bis(fullerenyl) groups at the termini of the oligomers. Spectroscopic and electrochemical properties of these novel bisfullerene triads were studied in detail by UV–vis, fluorescence, and cyclic voltammetric analyses, and the results of these investigations are reported.

There is a growing interest in fullerene (C_{60}) and π-conjugated oligomer hybrids, owing to their versatile applications in artificial photosynthesis, molecular optoelectronics, and nano-assemblies.[1] Especially, in organic photovoltaic cells, active components consisting of blends of organic conjugated polymers and C_{60} moieties can constitute 'bulk heterojunctions' which lead to considerably improved efficiency of light-to-current conversion.[2] Nevertheless, in these devices spontaneous phase segregation is a major setback that needs to be overcome. One way to deal with this problem is to covalently attach C_{60} groups to various oligomers. Therefore, the simple dyad motif, that is, C_{60}–oligomer, has been extensively adopted as a straightforward strategy for design of C_{60} based photovoltaic materials at the molecular level. More recently, sophisticated C_{60}–oligomer hybrid architectures, for instance, the dumbbell-shaped C_{60}–oligomer–C_{60} triad,[3] has emerged as an appealing design motif for functional C_{60}–oligomer hybrids. Although covalently incorporating multiple C_{60} cages into one molecule is synthetically challenging, the C_{60}–oligomer–C_{60} type of molecules have been found to show some advantageous properties and performance characteristics in comparison to the simple C_{60}–oligomer dyads. For example, enhanced stabilization effects of charge-separation (CS) state stemming from the second C_{60} group and better solid-state ordering could be achieved.[4]

In recent research, a number of electroactive linearly conjugated oligomers, including oligo(arylenevinylene)s,[5] oligo(phenylene ethynylene)s (OPEs),[6] and oligo(thiophene)s,[7] have been employed to serve as π-bridges for the C_{60}–oligomer–C_{60} molecular dumbbells. The nature of the central oligomer π-bridge can significantly affect electronic, optical, and photophysical properties.[3,5–7] However, the effects originating from conjugation pattern and dimensionality of the π-bridge are yet to be clarified due to lack of compounds whose π-bridge complexity is more than simple one-dimensional linear conjugation.

We report herein the first synthesis and property study of two novel C_{60}–oligomer–C_{60} triads **7** and **11**, in which cruciform-shaped OPE/OPV hybrid oligomers are enlisted as the bridging units instead of commonly used linear conjugated oligomers (Scheme 1). Analogous OPE/OPV cruciform oligomers were first investigated by Bunz's group[8] and showed intriguing electron delocalization characteristics and appealing applications in metal ion sensing. In our work, it was envisioned that adding two-dimensionally conjugated oligomer bridges (chromophores) in between two C_{60} groups would likely impart the molecule with interesting molecular behavior. Moreover, the cruciform bridge may also provide new access to multiple and versatile functionalization for fullerene-oligomer hybrids.

As outlined in Scheme 1, the synthesis of triads **7** and **11** began with a diiodophenylenevinylene building block **1**. Sonogashira coupling of **1** with 2 equiv of trimethylsilylacetylene (TMSA) afforded compound **2** in 87% yield.

* Corresponding authors. Tel.: +1 709 737 8046; fax: +1 709 737 3702 (D.W.T.); tel.: +1 709 737 8747; fax: +1 709 737 3702 (Y.Z.); e-mail addresses: dthompso@mun.ca; yuming@mun.ca

0040-4039/$ - see front matter
doi:10.1016/j.tetlet.2007.03.092

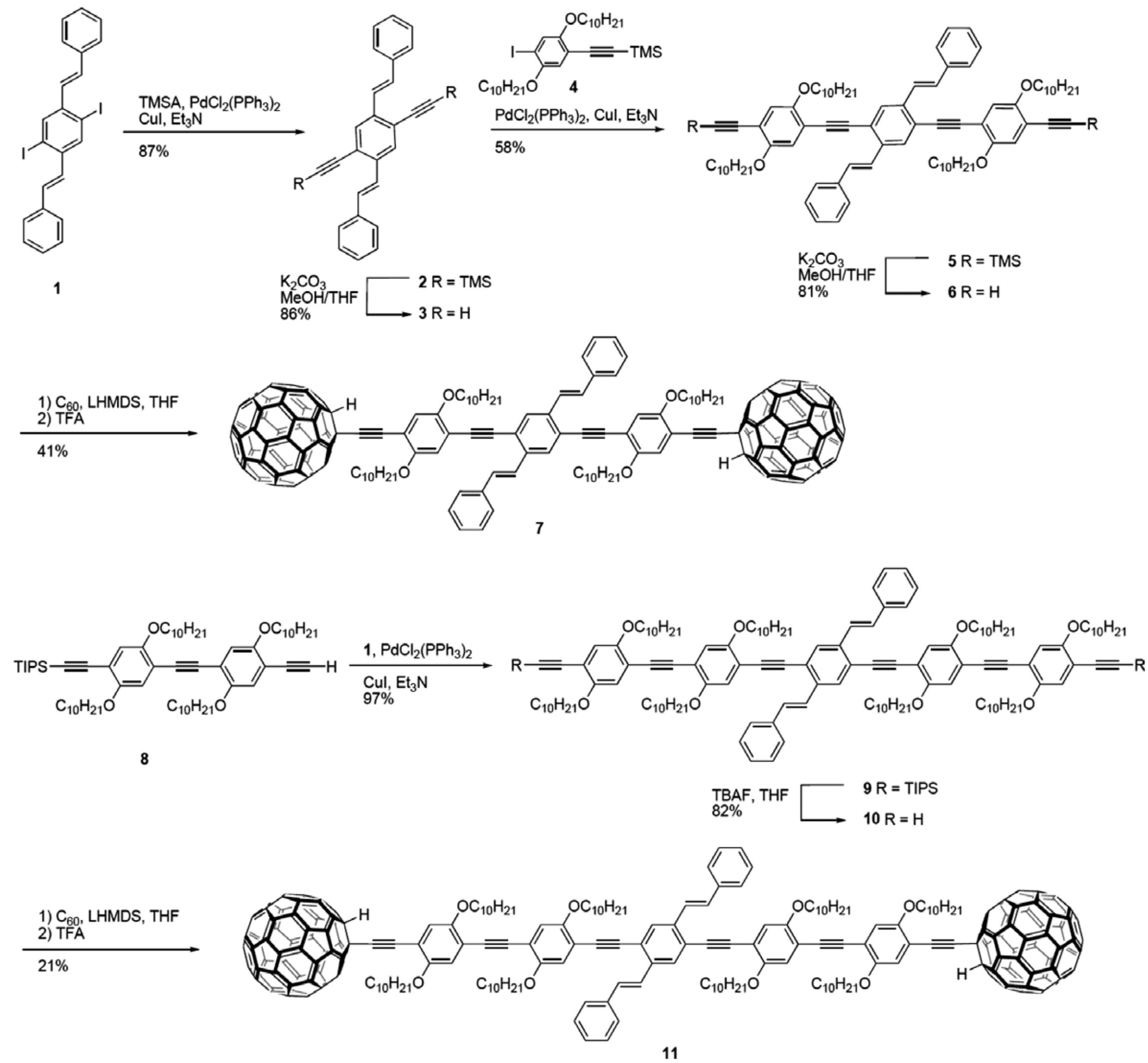

Scheme 1. Synthesis of cruciform oligomers and C_{60}–cruciform–C_{60} triads.

Compound **2** after protiodesilylation with K_2CO_3 was cross-coupled with iodoarene **4** to give TMS group end-capped cruciform oligomer **5**. Desilylation of **5** with K_2CO_3 yielded terminal alkyne **6**, which was immediately reacted with excess C_{60} via an in situ ethynylation reaction to afford triad **7** in a reasonable yield of 41%. In a similar manner, extended cruciform oligomers **9** and **10** were obtained via Sonogashira coupling and desilylation reactions. In situ ethynylation of C_{60} with **10** thus afforded another C_{60}–π–C_{60} triad **11** in 21% yield.

Molecular structures of the OPE/OPV cruciform oligomers and respective bisfullerenyl triads were clearly verified by spectroscopic analyses (detailed IR, NMR, and MS characterizations are provided in the Supplementary data).[9] The redox properties of triads **7** and **11** were characterized by cyclic voltammetry (CV) at room temperature. Detailed cyclic voltammograms and redox potential data are given in Figure 1 and Table 1. In spite of the presence of a cruciform π-bridge (supposedly a donor) in each of the molecules of **7** and **11**, their cyclic voltammograms give no meaningful oxidation features. In the negative potential region, distinctive reduction features were observed, however, the results of which were quite different from that observed in related C_{60}–OPE–C_{60} systems.[6c,d] The characteristic four reversible or quasi-reversible wave pairs ascribed to sequential

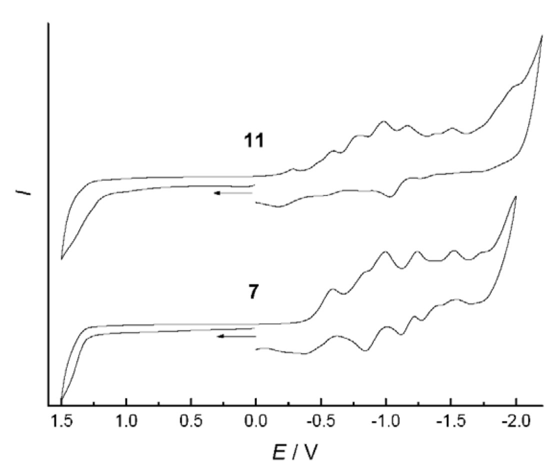

Figure 1. Cyclic voltammograms of triads **7** and **11**.

Table 1. Summary of electrochemical[a] and spectroscopic[b] properties of compounds **6**, **7**, **10** and **11** at room temperature

Entry	Reduction		Absorption		Emission			
	E_{pc}, V	E_{pa}, V	λ_{max}, nm (ε, M^{-1} cm^{-1})	Energy, cm^{-1}	λ_{em}, nm	Energy, cm^{-1}	Φ_{em}	Assignment
6	−1.67	−1.57	324 (5.8×10^4)	30,860	428	23,360		
			360 (7.8×10^4)	27,780	452 (sh)	22,120	0.96	π-Bridge
			390 (5.4×10^4, sh)	25,320				
7	−0.59, −0.85,	−0.38, −0.84,	254 (1.8×10^4, sh)	38,910	451	22,175		
	−1.00, −1.24,	−1.12, −1.27,	325 (9.4×10^3)	30,770	469 (sh)	21,320	~10^{-4}	π-Bridge
	−1.52, −1.73	−1.64	360 (8.7×10^3)	27,780	711	14,045		$^3C_{60}$ em
			403 (6.0×10^3, sh)	24,815				
10	−1.80	n/a	312 (2.1×10^4)	32,970	452	22,125		
			330 (2.4×10^4)	30,300	484 (sh)	20,660	0.96	π-Bridge
			372 (3.3×10^4)	26,890				
			410 (3.2×10^4, br)	24,390				
11	−0.29, −0.60,	−1.03	255 (2.6×10^5)	39,220	cf[c]		<0.01	π-Bridge
	−0.80, −0.99,		315 (1.5×10^5, sh)	31,950				
	−1.17, −1.51,		326 (1.6×10^5)	30,680				
	−1.97		370 (1.4×10^5)	27,030	711	14,045		$^3C_{60}$ em
			415 (1.3×10^5)	24,100				

[a] Redox properties were determined by cyclic voltammetry. Cyclic voltammograms were recorded in solutions of *o*-dichlorobenzene–CH_3CN (4:1). Bu_4NBF_4 (0.1 M) as the supporting electrolyte, glassy carbon as the working electrode, and platinum wire as the counter electrode. Potentials are given in volts versus a Ag/AgCl reference electrode. Scan rate: 100 mV s^{-1}.

[b] UV–vis spectra were obtained in N_2 saturated $CHCl_3$. Fluorescence spectra were measured in N_2 saturated toluene, uncorrected for instrument response.

[c] Obscured by emission from trace amounts of **10**.

reduction of functionalized C_{60} cage were not obvious in this case. Rather, triad **7** gives three characteristic quasi-reversible redox waves at $E_{1/2} = -0.48$, -0.92, and -1.20 V (vs Ag/AgCl) accompanied by two irreversible cathodic peaks ($E_{pc} = -0.85$ and -1.52 V vs Ag/AgCl) and one irreversible anodic peak ($E_{pa} = -1.27$ V vs Ag/AgCl). In the cyclic voltammogram of **11**, only one quasi-reversible wave appears at $E_{1/2} = -1.10$ V versus Ag/AgCl along with four irreversible cathodic peaks in the negative potential region. The origins of these irreversible reduction processes are not clear. However, these features are suggestive that the electronic interactions between the cruciform π-oligomer and C_{60} are more significant than those in the linear OPE bridged C_{60}–π–C_{60} system.[6]

UV–vis spectral data, extinction coefficients, emission spectral data, quantum yield, and optical energies are given in Table 1. Representative absorption and emission spectra for **6** and **7** are shown in Figure 2. Absorption spectra for **6** and **7** have a series of overlapping π→π* transitions localized on bridge in the 300–450 nm regime. These π→π* bands are superimposed transitions localized on the stilbene fragment, and the connecting phenylactylene moieties.[10] The absorption spectrum for **7** differs significantly from that observed for **6**. There is increased absorption below 300 nm and broad sloping shoulder that extends out past 700 nm. These transitions are associated with the C_{60} termini.[11] The transitions at 325 and 360 nm in **7** are also apparent in **6**, albeit the intensities of these absorption bands in **7** are smaller. The origin of the diminished intensity in **7** is not known and awaits a more detailed spectral deconvolution and theoretical analysis. Absorption spectra for **6** and **10** have a series of overlapping bridge localized π→π* transitions in the 300–450 nm regime. The ε_{max} values for **6** and **10** range from 2.0×10^4 to 7.8×10^4 M^{-1} cm^{-1} respectively, consistent with assignment of highly allowed $S_0 \rightarrow S_1$ transitions. Generally, the energies of the π→π* transitions are found at lower energies for **10** versus **6**, an expected observation based on the increased conjugation in **10** giving rise to more extended charge delocalization in **10**. Comparative spectra for **10** and

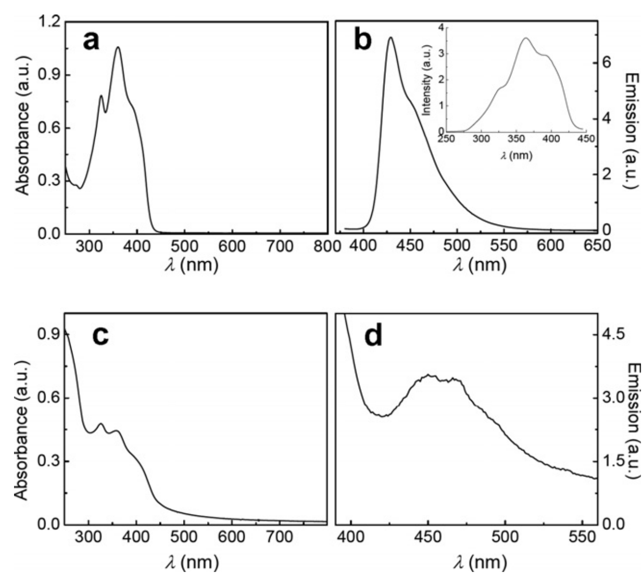

Figure 2. (a) UV–vis spectrum of **6**. (b) Fluorescence spectrum of **6** excited at 360 nm. Inset: excitation spectrum of **6**. (c) UV–vis spectrum of **7**. (d) Fluorescence spectrum of **7** excited at 320 nm.

11 follow the same trends as those described above for **6** and **7**, albeit the absorption spectral band intensities in **11** are higher than **10**, a trend that is reversed from observations made for **6** and **7**.

Emission spectra for **6** and **7** are shown in Figure 2. Emission from **6** at room temperature in N_2 saturated toluene shows a structured emission band envelope with a $\Phi_{em} = 0.96$ and possesses a lifetime of 2.8 ns ($k = 3.8 \times 10^8\ s^{-1}$) which is reasonably assigned as $S_1 \rightarrow S_0$ radiative transition. The excitation profile overlaps extensively with absorption spectra. However, the absorption band envelope and emission band envelope are not mirror images to each other, which is not surprising given that the absorption band envelope is composed of a series of $\pi\rightarrow\pi^*$ transitions localized on various light absorbing fragments in the bridge. The emission for **7** is more complex than that observed in **6**; the most intense emission transition of **7** occurs at 451 nm, some 1185 cm^{-1} lower in energy than **6**, with $\Phi_{em} \sim 10^{-4}$ for **7** versus 0.96 for **6**, and a new emission band appears beyond 700 nm. The emission at 711 nm is assigned to $^3C_{60}$ based emission based on comparison with analogous systems described elsewhere.[11] The attenuated bridge based emission in **7** is due to an additional non-radiative decay pathway(s), presumably energy transfer from the bridge giving rise to a $^3C_{60}$ emission and/or electron transfer quenching of the C_{60} termini based excited state by the bridge.[11,12] A similar behavior is apparent in **10** versus **11**. The exact nature of these decay pathways is under investigation and will be reported in a subsequent manuscript.

At this juncture, some qualitative comments on the relative photochemical stabilities of **1**, **6**, and **7** are useful. Light excitation into the absorption manifold of **1** result in facile changes in the emission and absorption spectra presumably due to trans→cis photo-isomerization of the stilbene based moiety.[12b] The photosensitivity of **6** is significantly attenuated, however, still occurs. For **7**, the trans→cis photo-isomerization is not observed to an appreciable extent, indicating rapid deactivation of the bridge based excited state via non-radiative decay processes alluded to in the previous paragraph.

In conclusion, we have prepared a series of novel cruciform shaped OPE/OPV hybrid oligomers and their bis(fullerenyl) endcapped derivatives, with their redox and photophysical properties well characterized. Two points are worth some final remarks here: (1) triads **7** and **11** show quite different electrochemical properties than other previously reported C_{60}–oligomer–C_{60} compounds. Likely, the relatively complex π-bridge structure have played a crucial role by exerting significant influence on factors such as electronic interactions and others; (2) the substantially quenched fluorescence of the bridge units in triads **7** and **11** is indicative of rapid photoinduced intramolecular energy/electron transfer, which may render these new fullerene-oligomer species potential candidates for advanced organic optoelectronic materials.

Acknowledgments

The authors thank NSERC Canada, the Canadian Foundation for Innovation (CFI), Industrial Research Innovation Fund (IRIF), and Memorial University of Newfoundland for funding. Professor C. Jablonski is acknowledged for funding of Li Wang. Dane Sheppard and Paul Inder are acknowledged for preliminary investigations.

Supplementary data

Supplementary data including synthetic details and spectroscopic characterizations for new compounds can be found in the online version, at doi:10.1016/j.tetlet.2007.03.092.

References and notes

1. For recent reviews of C_{60}/conjugated oligomer hybrids, see: (a) Segura, J. L.; Martín, N.; Guldi, D. M. *Chem. Soc. Rev.* **2005**, *34*, 31–47; (b) Nierengarten, J. F. *Sol. Energy Mater. Sol. Cells* **2004**, *83*, 187–199.
2. (a) Brabec, C. J.; Sariciftci, N. S.; Hummelen, J. C. *Adv. Funct. Mater.* **2001**, *11*, 15–26; (b) Marcos Ramos, A.; Rispens, M. T.; van Duren, J. K. J.; Hummelen, J. C.; Janssen, R. A. J. *J. Am. Chem. Soc.* **2001**, *123*, 6714–6715.
3. Sánchez, L.; Herranz, M. Á.; Martín, N. *J. Mater. Chem.* **2005**, *15*, 1409–1421, and references cited therein.
4. Sánchez, L.; Sierra, M.; Martín, N.; Guldi, D. M.; Wienk, M. W.; Janssen, R. A. J. *Org. Lett.* **2005**, *7*, 1691–1694.
5. (a) Segura, J. L.; Martín, N. *Tetrahedron Lett.* **1999**, *40*, 3239–3242; (b) Martineau, C.; Blanchard, P.; Rondeau, D.; Delaunay, J.; Roncali *J. Adv. Mater.* **2002**, *14*, 283–287; (c) Guldi, D. M.; Luo, C.; Swartz, A.; Gómez, R.; Segura, J. L.; Martín, N. *J. Phys. Chem. A* **2004**, *108*, 455–467.
6. (a) Atienza, C. M.; Fernández, G.; Sánchez, L.; Martín, N.; Dantas, I. S.; Wienk, M. M.; Janssen, R. A. J.; Rahman, G. M. A.; Guldi, D. M. *Chem. Commun.* **2006**, 514–516; (b) Atienza, C.; Insuasty, B.; Seoane, C.; Martín, N.; Ramey, J.; Aminur Rahman, G. M.; Guldi, D. M. *J. Mater. Chem.* **2005**, *15*, 124–132; (c) Zhao, Y.; Shirai, Y.; Slepkov, A. D.; Cheng, L.; Alemany, L. B.; Sasaki, T.; Hegmann, F. A.; Tour, J. M. *Chem. Eur. J.* **2005**, *11*, 3643–3658; (d) Shirai, Y.; Zhao, Y.; Cheng, L.; Tour, J. M. *Org. Lett.* **2004**, *6*, 2129–2132.
7. (a) van Hal, P. A.; Knol, J.; Langeveld-Voss, B. M. W.; Meskers, S. C. J.; Hummelen, J. C.; Janssen, R. A. J. *J. Phys. Chem. A* **2000**, *104*, 5974–5988; (b) Dhanabalan, A.; Knol, J.; Hummelen, J. C.; Janssen, R. A. J. *Synth. Met.* **2001**, *119*, 519–522.
8. (a) Wilson, J. N.; Bunz, U. H. F. *J. Am. Chem. Soc.* **2005**, *127*, 4124–4125; (b) Wilson, J. N.; Smith, M. D.; Enkelmann, V.; Bunz, U. H. F. *Chem. Commun.* **2004**, 1700–1701; (c) Wilson, J. N.; Josowicz, M.; Wang, Y.; Bunz, U. H. F. *Chem. Commun.* **2003**, 2962–2963.
9. The purities of all new compounds were satisfactory enough to give trustworthy electrochemical, UV–vis and fluorescence spectroscopic results, except the emission of **11**.
10. Spectral data for **1** in toluene: UV–vis: 299 nm (33,445 cm^{-1}), 310 nm (32,260 cm^{-1}); emission: 338 nm

(29,590 cm^{-1}), 352 nm (28,410 cm^{-1}), 375 nm (26,679 cm^{-1}). Spectral data for **4** in toluene: UV–vis: 331 nm (30,210 cm^{-1}), sh 344 nm (29,070 cm^{-1}); emission: 370 nm (27,030 cm^{-1}).

11. Guldi, D. M.; Prato, M. *Acc. Chem. Res.* **2000**, *33*, 695–703.

12. (a) Excitation at 263 nm, a transition localized on the C_{60} cage does not give rise to a bridge-based emission. (b) Note that the cis–trans isomerization hypothesis will be elaborated on in a subsequent manuscript.